This paper is based on a thesis submitted by one of us (M.A.N.) in partial fulfillment of the requirements for the degree of Master of Science at the University of Arkansas.

[1]M. D. Crisp, Phys. Rev. Lett. 22, 820 (1969).
[2]J. H. Eberly, Phys. Rev. Lett. 22, 760 (1969).
[3]D. Dialetis, Phys. Rev. A 2, 1065 (1970).
[4]L. Matulic and J. H. Eberly, Phys. Rev. A 6, 822, 1258 (1972).
[5]S. L. McCall and E. L. Hahn, Phys. Rev. 183, 457 (1969).
[6]With an appropriate redefinition of the field, all equations and results in this Letter also apply to a $\Delta m = \pm 1$ transition.
[7]G. L. Lamb, Jr., Rev. Mod. Phys. 43, 99 (1971).
[8]The difference between any two particular solutions to the inhomogeneous linear differential equations (2) is a solution to the corresponding homogeneous equations. It is straightforward to show that for any solution to the homogeneous equations, the magnitude decays aways as in Eq. (3).
[9]Ref. 4, Eqs. (3.17)–(3.19). With $(T_1)^{-1} = (T_2')^{-1} = 0$, Eqs. (2) describe a pure rotation. The repetitive unit Bloch vector is therefore unique (up to a sign) since it must lie along the axis of the rotation representing one period. An exception occurs at values of $\Delta\omega$ such that this rotation is a multiple of $2\pi$. However, if the atomic line shape is nonsingular, the Bloch vectors at these discrete $\Delta\omega$'s cannot contribute to the $\Delta\omega$ averaging in Eqs. (1) and thus can be ignored.

# Measurement of Return Current in a Laser-Produced Plasma

Robert F. Benjamin, Gene H. McCall, and A. Wayne Ehler
*Los Alamos Scientific Laboratory, University of California, Los Alamos, New Mexico 87545*
(Received 15 December 1978)

A laser-fusion target's support fiber is heated at large distances from the laser plasma principally by Ohmic heating due to an electrical return current. Optical and electrical measurements demonstrate that return-current heating dominates over other heating mechanics such as hot-electron propagation along the fiber, thermal conduction, and line-of-sight plasma radiation.

Much attention has been directed toward the problem of energy flow into the interior of laser-produced plasmas,[1-3] but little work has been done on the problem of lateral energy conduction in the target and its support structure.[4,5] Transverse energy flow can improve the symmetry of energy deposition in a laser-fusion target, but it can also conduct energy away from the focal region through support structures and modify the hot-electron spectrum.[6] It may also affect the interpretation of laser-plasma experiments, such as shock generation.[5,7,8] Several theoretical and experimental studies indicate that the effective energy density in the focal region may be reduced as a result of a large lateral energy flow.[3-5,9] Although this reduced intensity can be used to interpret such experiments as foil burnthrough,[1-3,9] no mechanism that justifies this assumption has been proposed.

We report results of an experiment that determines the dominant mechanism for heating due to lateral energy flow along a support fiber at large distances (i.e., more than several focal radii) from the laser-produced plasmas. The dominant mechanism is Ohmic heating due to electrical return current that is driven by hot-electron emission from the laser-produced plasma. We found that the return-current heating may deposit a significant amount of energy relative to other support-fiber–heating mechanisms at large distances from the focal region. This energy deposition is usually a small portion of the energy absorbed at the target.

We determined the importance of return-current heating by measuring its dominance over three other mechanisms of lateral heat flow: (1) thermal conduction (i.e., a thermal wave with no flow of electrical current), (2) plasma radiation (i.e., line-of-sight irradiation by particles or photons emitted from the plasma), and (3) hot-electron propagation along the support structure. An optical experiment discriminated between heating by electrical current, thermal wave, and plasma radiation, while an electrical measurement distinguished between heating by return current and hot-electron propagation. The optical experiment also demonstrated that scattered laser radiation does not significantly heat the support fiber.

These experiments are described below and further detail will be presented in a subsequent comprehensive article. Following the experimental details we discuss an analytical model that interprets the data.

The optical experiment consists of a relatively complex target with simple diagnostics. The basic target design consists of a tortuous path of 10-$\mu$m-diam glass fibers. The fibers provide alternative paths of energy flow from the laser-irradiated region to the massive target holder attached to the chamber ground. The target is shown schematically in Fig. 1(a). A single beam of the Los Alamos Scientific Laboratory's Gemini (two-beam) $CO_2$-laser system irradiated the target with a 300-J, 1.2-ns full width at half maximum (FWHM), 10.6-$\mu$m-wavelength light pulse having an intensity of $3\times10^{15}$ W/cm$^2$. The laser beam impinges on a glass microballoon at location $A$.

The principal plasma diagnostic was a time-integrated optical photograph of the self-luminous target. The axis of the $f/15$ camera was 14° from the incident laser-beam's direction. Typical data are shown in Figs. 1(b) and 1(c). The large luminous region is plasma blowoff from the shield $K$, believed to be unimportant here. The critical observations involve relative luminosities of the fiber segments.

The results indicate that heating by an electrical current dominates heating by a propagating thermal wave, by plasma radiation, and by scattered laser light. The target shown in Fig. 1(b) had fiber $J$ present, but this fiber was absent in the target of Fig. 1(c). One clearly sees that the most luminous path is from the irradiated region to the nearest ground (i.e., the massive target holder). We exclude purely thermal conduction as the dominant mechanism by observing that in Fig. 1(b) the heat flow follows the ground path $J$ rather than the alternative path $D$. Similarly, we assert the insignificance of plasma radiation and scattered laser light by observing that region $D$, which was protected from plasma emissions and scattered light by the shield $K$, is not luminous in Fig. 1(b), but it is quite bright in Fig. 1(c). However, plasma radiation may produce heating as evidenced by the luminosity of segment $H$. The greater width of this segment's image, a result of expansion, indicates either that its heating occurs later than the heating of segments $B$ and $C$ or that scattered laser light heats its low-density blowoff.

These results indicate the importance of an electrical current. To obtain quantitative results and to distinguish between hot-electron flow —which is balanced by an opposing current—and hot-electron emission into vacuum, we measured current flowing in the target's support structure. An aluminum target 12 mm×15 mm×6 mm thick was mounted at the end of the center conductor of an RG-223 50-Ω coaxial cable, and the outer conductor was grounded to the target chamber. The aluminum slab was illuminated with 133 J of $CO_2$ laser light on a 1.2-ns-FWHM pulse in a focal area of $7.9\times10^{-5}$ cm$^2$. The voltage was measured with a 5-GHz-bandwidth oscilloscope and 119 dB of wide-bandwidth attenuation was placed between the oscilloscope and the target. The observed electrical pulse, shown in Fig. 2, was positive, indicating a net flow of electrons toward the target region (i.e., the conventional current flows from target to oscilloscope). Therefore, the electrical current in the support fibers is the return

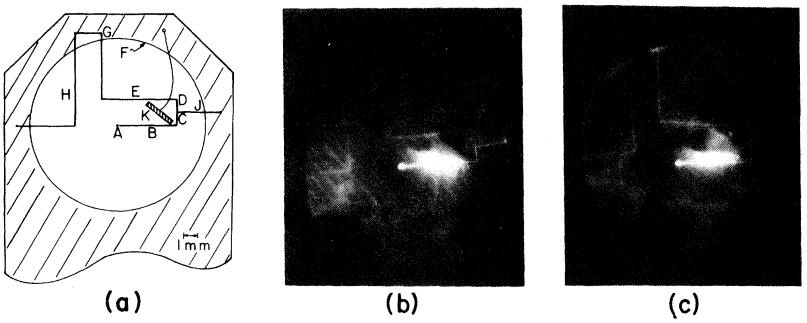


FIG. 1. The target shown schematically in (a) produced the time-integrated optical photographs in (b) and (c). The fibers are coplanar, but the massive shield $K$ extends out of the plane. In (c) the fiber $J$ was intentionally absent. Note that the most luminous regions extend from the glass microballoon at position $A$ to the nearest ground.

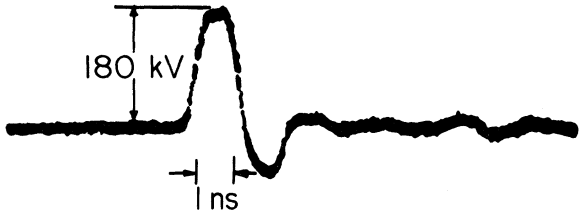


FIG. 2. This oscillograph of the target's voltage demonstrates a net return current.

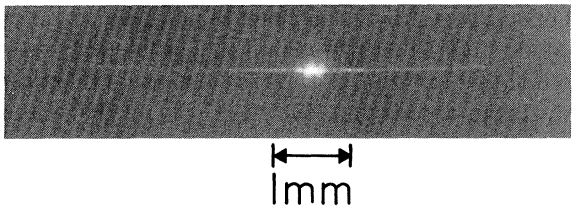


FIG. 3. This x-ray photograph of a single irradiated fiber shows that significant energy is transported many focal radii from the laser-irradiated region.

current. The peak voltage was 175 kV.

The effect of return-current heating on lateral conduction can be seen in Fig. 3. A 1-cm-long, 10-$\mu$m-diam glass fiber was illuminated at its center by a laser pulse as described above. Figure 3 is an x-ray pinhole-camera photograph of the fiber emission in the 1–2-keV range. The brightness of the fiber implies a temperature of ~100 eV, and the heated region at the center of the fiber extends for ~400 $\mu$m although the focal-spot diameter was <100 $\mu$m. The increased area of the heated region can, therefore, reduce the energy density by a factor of 5 to 10 for extended targets. The precise role of the return current is not well understood; it may provide the heating directly or prepare an energy-deposition path for another mechanism.[9] The bright spots along the fiber are not well understood, but they are consistent with a "sausage" instability driven by current flow along the surface of the fiber.[10] The fiber target demonstrates these effects more graphically than an infinite-plane target because it approximates a linear system where the temperature varies as $1/d$ rather than $1/d^2$, where $d$ is the distance from the laser-produced plasma.

Energy deposition from current flow in a laser-heated target can be estimated from a simple model of electron emission into vacuum from the laser focal spot,[11] which is balanced by a return current flow. The model yields a useful scaling relation as well as estimate of the voltage pulse. We assume a Maxwellian hot-electron distribution $f(u)$, at a temperature $T$, given by[6]

$$T=\alpha(\varphi\lambda^2)^{1/3}, \tag{1}$$

where $\varphi$ is the laser intensity and $\lambda$ is the wavelength. For $\varphi$(W/cm$^2$)$\lambda^2$($\mu$m) expressed in units of $10^{17}$ W $\mu$m$^2$/cm$^2$ and $T$ in keV, $\alpha\approx 30$. This is the internal distribution, which is not necessarily that of Ref. 11. The emitted-hot-electron current $I$ is

$$I=neA\int_{u_1}^{\infty} uf(u)\,du, \tag{2}$$

where $u_1=(2V_0e/m)^{1/2}$, $A$ is the area of the laser focal spot, $n$ is the hot-electron density, $u$ is the electron velocity, $V_0$ is the target potential, $e$ is the electron charge, and $m$ is the electron mass. It should be noted that $V_0$ is not necessarily the potential of the target substrate because of sheath fields, but for $eV_0\gg kT$ the sheath potentials can be ignored. Charge continuity and small target size, however, guarantee that the emitted current and the substrate current are equal. Measurements of substrate potential for an isolated target have been reported by Pearlman and Dahlbacka[12] and for a grounded target by Ehler.[13]

Using Eq. (1) and equating the hot-electron flux to the absorbed laser flux, we implicitly calculate $n$ from

$$a\varphi=\tfrac{1}{2}nm\int_0^{\infty}u^3f(u)\,du, \tag{3}$$

where $a$ is the fraction of the laser intensity absorbed. Combining Eqs. (1) through (3) and evaluating the integral, one obtains an expression for the hot-electron current that is equal to the return current. Assuming that the fiber or substrate can be characterized by a resistance $R$ and that sheath potentials are negligible, the target potential $V_0$ (in kilovolts) is given by

$$V_0=IR=\frac{0.464aP^{2/3}A^{1/3}R\exp(-V_0/T)}{\alpha\lambda^{2/3}}, \tag{4}$$

where $P=\varphi A$ is the measured laser power in watts. For a 10-$\mu$m-diam glass fiber with a length of 5 mm at a temperature of 100 eV, assuming a strong magnetic field,[14] the resistance is ~50 $\Omega$. The inductance is ~7 nH, which gives a time constant $L/R\sim 140$ ps, which is much less than the laser pulse. Inductive effects can therefore be ignored. For the conditions of the aluminum-slab experiment, with $a=0.3$,[15] $P=1.1\times10^{11}$ W, $T=33.5$ keV from Eq. (1), and $R=50$ $\Omega$, the estimated value of $V_0$ is 187 kV, which is in good

agreement with the experimental value of 175 kV. Measurements at lower power were consistent with $P^{2/3}$ scaling, suggesting the usefulness of Eq. (4) as a scaling relation.

We conclude that the observed heating of the target's support structure at large distances is dominantly the Ohmic heating caused by the return electron current. The description of the hot-electron–driven return current given above also implies that the electrons on the high-energy tail of the Maxwellian electron distribution are emitted, thereby modifying the distribution function in the plasma. These reported measurements should be useful in modifying computer simulations that presently lack net return-current flow. The magnitude of the net current flow is large enough to affect magnetic field distributions that have been reported in laser-heated targets.

We are grateful to David B. vanHusteyn for the x-ray photography and we appreciate the technical assistance of Jim Riffle, Betty Cranfill, Verna Woods, and Vivian Gurule and the laser staff. We acknowledge useful discussions with Robert P. Godwin, Damon V. Giovanielli, Charles W. Cranfill, Eldon Linnebur, and S. J. Gitomer. This work was performed under the auspices of the U. S. Department of Energy.

[1]A. W. Ehler, D. V. Giovanielli, R. P. Godwin, G. H. McCall, R. L. Morse, and S. D. Rockwood, LASL Report No. LA-5611-MS, 1974 (unpublished).

[2]R. C. Malone, R. L. McCrory, and R. L. Morse, Phys. Rev. Lett. 34, 721 (1975).

[3]S. J. Gitomer and D. B. Henderson, to be published.

[4]M. H. Key, K. Eidmann, C. Dorn, and R. Sigel, Phys. Lett. 48A, 121 (1974).

[5]C. G. M. van Kessel and R. Sigel, Phys. Rev. Lett. 33, 1020 (1974).

[6]D. W. Forslund, J. M. Kindel, and K. Lee, Phys. Rev. Lett. 39, 284 (1977).

[7]L. R. Veeser and J. C. Solem, Phys. Rev. Lett. 40, 1390 (1978).

[8]R. J. Trainor, J. W. Shaner, J. M. Auerbach, and D. W. Phillion, Lawrence Livermore Laboratory Report No. UCRL-80257, 1978 (unpublished).

[9]H. Shay, G. Zimmerman, and J. Nuckolls, Lawrence Livermore Laboratory Report No. UCRL-75883, 1974 (unpublished), and Bull. Am. Phys. Soc. 19, 868 (1974).

[10]S. Chandrasekhar, *Hydrodynamic and Hydromagnetic Stability* (Clarendon Press, Oxford, 1961).

[11]D. V. Giovanielli, J. F. Kephart, and A. H. Williams, Appl. Phys. Lett. 47, 2907 (1976).

[12]J. S. Pearlman and G. Dahlbacka, Appl. Phys. Lett. 31, 414 (1977).

[13]A. W. Ehler, Bull. Am. Phys. Soc. 21, 1064 (1976).

[14]L. Spitzer, *Physics of Fully Ionized Gases* (Interscience, New York, 1956).

[15]V. M. Cottles, Bull. Am. Phys. Soc. 22, 1090 (1977).

# Extended Fine Structure on the Carbon Core-Ionization Edge Obtained from Nanometer-Sized Areas with Electron-Energy-Loss Spectroscopy

P. E. Batson[a]

*Department of Natural Philosophy, University of Glasgow, Glasgow G12 8QQ, Scotland*

and

A. J. Craven[b]

*Cavendish Laboratory, University of Cambridge, Cambridge CG3 0HE, England*

(Received 4 October 1978)

Extended fine structure, equivalent to extended x-ray–absorption fine structure, has been observed on carbon $K$-ionization edges obtained with electron energy-loss spectroscopy utilizing 0.75- to 5-nm radius probe sizes, and sampling as few as $10^4$ atoms in times as short as 4 min. Radial distribution functions show the expected behavior for graphite and an amorphous carbon sample. A second "amorphous" sample, however, shows structure which suggests the existence of local tetrahedral coordination.

There has been interest recently in the use of the inelastic scattering of fast electrons (electron-energy-loss spectroscopy or EELS) as a probe of the inner core excitations of materials to determine electronic band structure[1,2] and area-averaged structural information from extended electron-energy-loss fine structure (EXELFS)[3-6] equivalent to extended x-ray–absorption fine structure (EXAFS) in the photon absorption experiment. In addition, it has been re-

 

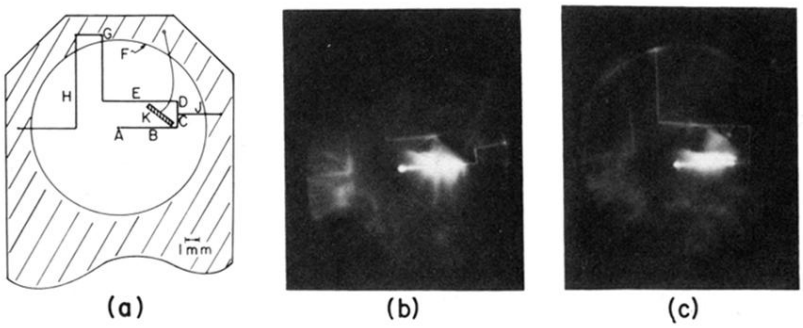


FIG. 1. The target shown schematically in (a) produced the time-integrated optical photographs in (b) and (c). The fibers are coplanar, but the massive shield *K* extends out of the plane. In (c) the fiber *J* was intentionally absent. Note that the most luminous regions extend from the glass microballoon at position *A* to the nearest ground.

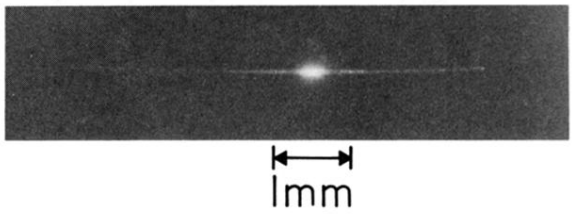


FIG. 3. This x-ray photograph of a single irradiated fiber shows that significant energy is transported many focal radii from the laser-irradiated region.